Journal of Bioenergetics and Biomembranes, Vol. 37, No. 2, April 2005 (© 2005)
DOI: 10.1007/s10863-005-4129-7

Manipulating the Length of the *b* Subunit F_1 Binding Domain in F_1F_0 ATP Synthase from *Escherichia coli*

Deepa Bhatt,[1] Stephanie P. Cole,[1] Tammy Bohannon Grabar,[1] Shane B. Claggett,[1] and Brian D. Cain[1,2]

Received January 31, 2005; accepted February 17, 2005

The peripheral stalk of F_1F_0 ATP synthase is composed of a parallel homodimer of *b* subunits that extends across the cytoplasmic membrane in F_0 to the top of the F_1 sector. The stalk serves as the stator necessary for holding F_1 against movement of the rotor. A series of insertions and deletions have been engineered into the hydrophilic domain that interacts with F_1. Only the hydrophobic segment from val-121 to ala-132 and the extreme carboxyl terminus proved to be highly sensitive to mutation. Deletions in either site apparently abolished enzyme function as a result of defects is assembly of the F_1F_0 complex. Other mutations manipulating the length of the sequence between these two areas had only limited effects on enzyme function. Expression of a *b* subunit with insertions with as few as two amino acids into the hydrophobic segment also resulted in loss of F_1F_0 ATP synthase. However, a fully defective *b* subunit with seven additional amino acids could be stabilized in a heterodimeric peripheral stalk within a functional F_1F_0 complex by a normal *b* subunit.

KEY WORDS: ATP synthase; *b* subunit; F_1F_0.

INTRODUCTION

F_1F_0 ATP synthases share a common overall structure and rotary mechanism (Noji and Yoshida, 2001; Boyer, 2002; Senior *et al*., 2002). Energy from translocating protons down an electrochemical gradient across a membrane provides the driving force for ATP synthesis. In the *Escherichia coli* enzyme, the F_1 sector consists of a hexamer of $\alpha_3\beta_3$ subunits with the three catalytic sites housed in the subunit interfaces. The $\gamma\varepsilon$ subunits form the rotor stalk that spans from the membrane surface up through the center of the $\alpha_3\beta_3$ hexamer. The rotor stalk sits atop a ring of approximately 10 *c* subunits in the F_0 sector. The *a* subunit lies alongside the *c* ring in the membrane and contains much of the F_0 proton channel. Protonation–deprotonation of the *c* subunits results in generation of torque on the rotor. Rotation of the rotor drives the conformational changes in the catalytic sites that account for enzyme's properties described by the binding change mechanism. The function of the peripheral stalk is to hold the $\alpha_3\beta_3$ against this rotation.

The peripheral stalk consists of the δ subunit and a b_2 dimer. The δ subunit is stably anchored to the amino-terminal domain of a single α subunit near the very top of the F_1 sector (Ogilvie *et al*., 1997; Weber *et al*., 2003, 2004). The two *b* subunits exist in a parallel arrangement extending from the periplasmic side of the membrane all the way to make direct protein–protein contact with the δ subunit (Dunn *et al*., 2000a; Cain, 2000; Wilkens, 2000). Nuclear magnetic resonance studies of a polypeptide modeling the membrane domain suggested an α-helical secondary structure (Dmitriev *et al*., 1999). Crosslinking (Dmitriev *et al*., 1999) and mutagenesis (Hardy *et al*., 2003) experiments indicated a close association between the *b* subunits on the periplasmic leaflet of the membrane, but that the two subunits may flare apart as the membrane is traversed. To date, no high resolution structure is available for the tether domain that stretches from the membrane surface to the bottom of the F_1 sector. However, deletion and insertion studies suggested that the tether domain is quite flexible (Sorgen *et al*., 1998, 1999).

[1] Department of Biochemistry and Molecular Biology, University of Florida, Gainesville, Florida 32605.
[2] To whom correspondence should be addressed; e-mail: bcain@biochem.med.ufl.edu.

Indeed, functional F_1F_0 complexes could be assembled that contained heterodimeric peripheral stalks with the *b* subunits differing in the lengths of their tether domains (Grabar and Cain, 2003).

The *b* subunit dimerization domain forms a segment of the peripheral stalk lying alongside F_1. Dunn and coworkers (2000a) have performed a series of studies demonstrating that the region from ala-55 to lys-122 was required for *b* dimer formation. A polypeptide modeling this region of the *b* subunit readily formed dimers in solution. A high resolution structure of monomers of the polypeptide revealed an α-helix in an essentially linear conformation (Del Rizzo *et al*., 2002). The hydrophobic val-124 to ala-132 segment is located at the junction of the dimerization and F_1 binding domains. Missense mutations $b_{ala128\rightarrow asp}$ and $b_{gly131\rightarrow asp}$ severely affected enzyme assembly (Porter *et al*., 1985; Howitt *et al*., 1996; Dunn *et al*., 2000b). The F_1 binding domain extends out to the carboxyl terminus of the *b* subunits and participates in a direct protein–protein interaction with the δ subunit (McLachlin *et al*., 1998; McLachlin and Dunn, 2000). Close interactions between *b* subunits were detected in the F_1 binding domain, but these were not absolutely required for the dimerization. Deletion of as few as four amino acids from the carboxyl terminus of the *b* subunit ($b_{\Delta val153-leu156}$) eliminated interaction with subunit δ and destroyed enzyme function (Takeyama *et al*., 1988). Recently, Motz *et al*. (2004) reported an elegant site-specific electron spin resonance study characterizing subunit interactions between the *b* subunits and with F_1.

In the present study, we continue the use of the insertion and deletion mutagenesis approach to consider sequence constraints in the dimerization and F_1 binding domains of the *b* subunit. Most manipulations of subunit length had limited impacts on F_1F_0 ATP synthase function. As expected, the hydrophobic segment and carboxyl terminus proved particularly sensitive to mutation resulting in major defects in F_1F_0 assembly. However, a defective *b* subunit could be stabilized within active F_1F_0 complexes by association with a normal *b* subunit.

EXPERIMENTAL PROCEDURES

Bacterial Strains, Mutagenesis and Growth Conditions

E. coli strain KM2 (Δb) carrying a deletion engineered in the chromosomal copy of the *uncF*(*b*) gene was used as the host strain for all experiments (McCormick and Cain, 1991). The mutations requiring insertion or deletion of four or fewer codons were constructed in plasmid pKAM14 (*b*) that expressed a wild type *b* subunit using the QuikChange Mutagenesis kit (Stratagene) using the oligonucleotides shown in Fig. 1. Larger insertions were constructed by cassette mutagenesis (Sorgen *et al*., 1999) using BssHII and BglII restriction sites engineered at nucleotides 346–351 and 374–379, respectively. In every case, a restriction endonuclease site was engineered to facilitate identification of recombinant plasmids. All mutations were confirmed by direct nucleotide sequencing of the entire *uncF*(*b*) gene on the plasmids. Strain KM2 (Δb) was made competent for transformation by treatment with $CaCl_2$ and transformed by standard protocols. Transformants were selected by screening for resistance to ampicillin. Culture media were purchased from Difco and antibiotics and other chemicals were obtained from Sigma. Minimal A medium containing succinate (0.2% w/v) as the sole carbon source and ampicillin (100 μg/mL) was used to score for growth via oxidative phosphorylation (Miller, 1992). LB glucose (0.2% w/v) ampicillin (100 μg/mL) was used for experiments involving membrane preparation. All growth experiments were carried out at 37°C.

Preparation of Membranes

Membrane vesicles were prepared by the method of Caviston *et al*. (1998). Bacterial cultures were grown to a density of approximately $OD_{600} = 1.0$. The cells were collected by centrifugation ($12{,}000 \times g$, 10 m) and washed with TM buffer (50 mM Tris–HCl, 10 mM $MgSO_4$, pH 7.5). The cells were suspended in TM buffer with DNaseI added to a concentration of (10 μg/mL). Cells were broken in a French Pressure Cell at (14,000 psi). Two sequential centrifugation steps ($7700 \times g$, 10 m) were performed to remove particulates. Membrane vesicles were recovered by centrifugation ($150{,}000 \times g$, 1.5 h) and then washed with TM buffer ($150{,}000 \times g$, 1 h) using a Beckman Coulter LE-80K ultracentrifuge with a 70.1 Ti rotor. The membranes were carefully suspended in TM buffer using a glass homogenizer with a teflon pestle. Membrane protein was determined by the standard methods (Smith *et al*., 1985). Experiments involving preparation of F_1F_0 complexes with heterodimeric stalks were performed as previously described (Grabar and Cain, 2003, 2004). Membrane samples (5 mg protein) were diluted to 1 mL in 0.2% tegamineoxide WS-35, 0.15 M NaCl, and 1 mM imidazole. Complexes containing amino terminal histidine-tagged *b* subunits (b_{6his}) were then collected by the batch preparation method using nickel chelate affinity matrix (Ni-CAM) purchased from Sigma.

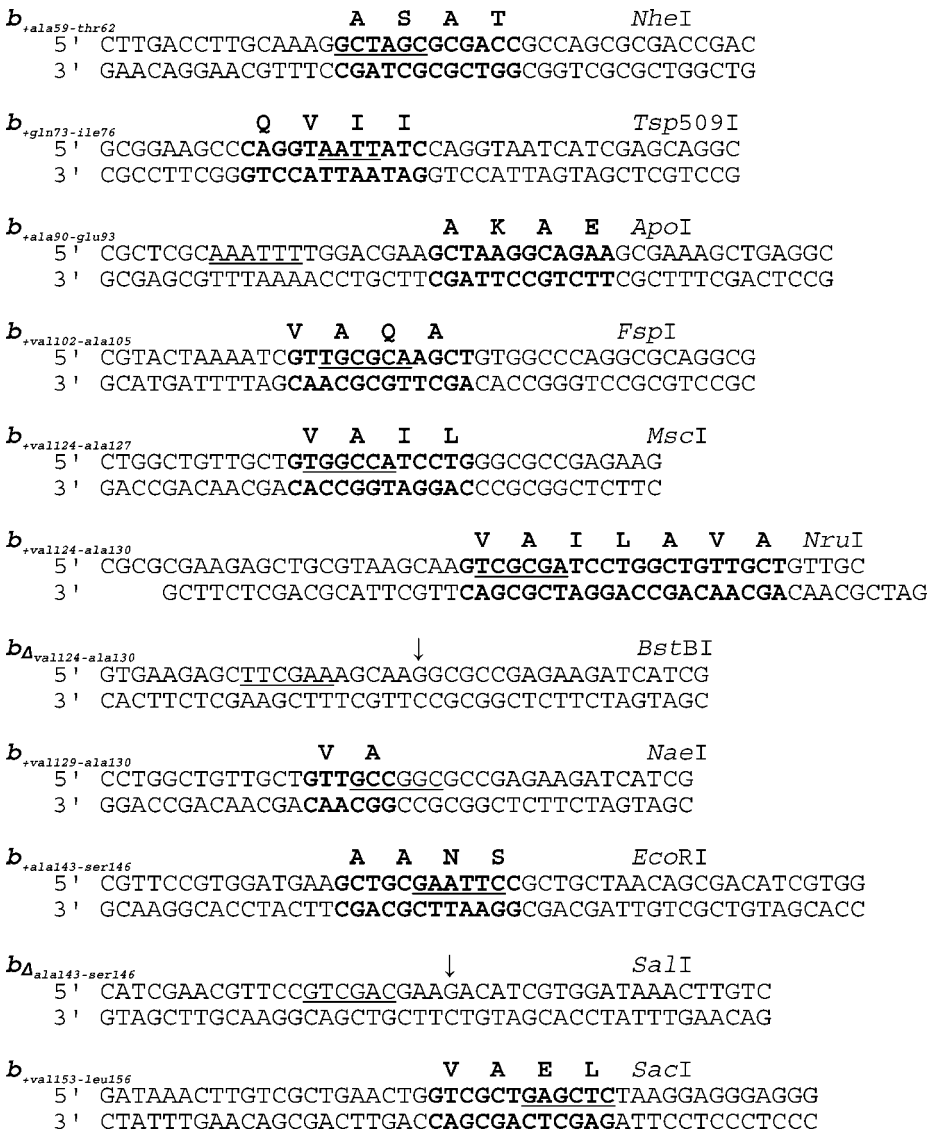

Fig. 1. Mutagenic oligonucleotides. The pairs of oligonucleotides used to generate novel mutations for this study are shown annealed in anti-parallel orientations. Most mutations were constructed with perfectly complementary primers using the QuikChange (Stratagene) mutagenesis kit. The $b_{\Delta val124-ala130}$ was made using cassette mutagenesis, so the oligonucleotides were designed with BssHII and BglII sticky ends. For each pair of oligonucleotides the mutation (single letter code), inserted bases (bold) and the restriction endonuclease (underline) used to detect recombinant plasmids are indicated. The positions of deletions are shown with arrows (↓).

Biochemical Assays

ATP hydrolysis was determined in membrane vesicles by monitoring the release of inorganic phosphate from ATP via the acid molybdate method (Sorgen *et al*., 1999). Lauryl dimethylamine oxide (LDAO) stimulated ATPase activity was determined by the method of Gardner and Cain (1999). Reactions were routinely done with 60 μg membrane protein suspended in 4 mL reaction buffer (50 mM Tris–HCl, 1 mM $MgCl_2$, pH 9.1, 37°C). The reaction was initiated by addition of ATP (80 μL of 150 mM ATP in 25 mM Tris–HCl, pH 7.5). ATP and NADH driven proton pumping assays were conducted by monitoring fluorescence of 9-amino-6-chloro-2-methoxyacridine (ACMA) as previously detailed (Sorgen *et al*., 1998). Separation of membrane proteins was achieved on 15%

SDS-PAGE gels (BioRad). Immunoblot analyses were conducted using the ECL enhanced chemiluminescence system as described by Grabar and Cain (2003, 2004).

RESULTS

Construction of Mutations

Construction of insertion and deletion mutations in the tether domain of the *b* subunit suggested considerable flexibility with respect to the length of the subunit (Sorgen *et al*., 1998, 1999). However, since the dimerization and F_1 binding domains are in contact with F_1 it seemed reasonable that insertions and deletions throughout these areas might perturb important subunit interactions. Therefore, a series of insertions and deletions were constructed at semi-regular intervals (Fig. 2). The carboxyl half of the *b* subunit is thought to have largely α-helical secondary structure (Fig. 2), so four codon mutations were generated to approximate single turns of an α-helix maintaining the orientation of the two *b* subunits relative to each other. The hydrophobic sequence val124 to ala132 was already known to be sensitive to single amino acid substitution mutations so several different insertions and deletions were constructed at that location. All mutations were constructed in the *b* subunit expression plasmid pKAM14 (*b*), and then transformed into *E. coli* strain KM2 (Δb) that has a chromosomal deletion in the *uncF*(*b*) gene. Therefore, the only *b* subunits present were from the recombinant plasmids, and function could be assessed by complementation analysis.

Growth of Mutants

Growth on succinate-based minimal medium was used as an initial assay of F_1F_0 ATP synthase function (Table I). The dimerization domain insertions $b_{+\text{ala59-thr62}}$, $b_{+\text{gln73-ile76}}$, $b_{+\text{ala90-glu93}}$, and $b_{+\text{val102-ala105}}$ all grew well on succinate medium.

Closer to the carboxyl terminus, several mutations resulted in readily detectable deficiencies. As expected, the carboxyl terminal truncation $b_{\Delta\text{val153-leu156}}$ resulted in a F_1F_0 ATP synthase defective phenotype (Table I). Similarly all of the manipulations of the hydrophobic sequence including the two amino acid insertions $b_{\text{val129-ala130}}$ also resulted in loss of growth. Large insertions, such as duplicating seven codons in the $b_{+\text{val124-ala130}}$ mutant, frequently gave rise to a few large, apparently healthy colonies when grown on selective minimal medium. Restriction endonuclease digestions of DNA prepared from these colonies showed that the marker restriction sites included during construction of the insertions had been retained. However, nucleotide sequence analysis showed that rearrangements had occurred resulting in reversion to a single copy of the val124 to ala130 segment and restoration of a coding sequence yielding a wild type *b* subunit. The $b_{+\text{val124-ala130}}$ duplication mutants were the most unstable mutations that we have encountered among the many mutations constructed in the F_1F_0 ATP synthase genes. Duplicating the four amino acids at the carboxyl terminus in the $b_{+\text{val153-leu156}}$ or addition of the V5 epitope tag (Grabar and Cain, 2003) did not affect growth. In summary, only changes to the hydrophobic sequence at the junction of dimerization and F_1 binding domains or deletion of the carboxyl terminus $b_{\Delta\text{val153-leu156}}$ resulted

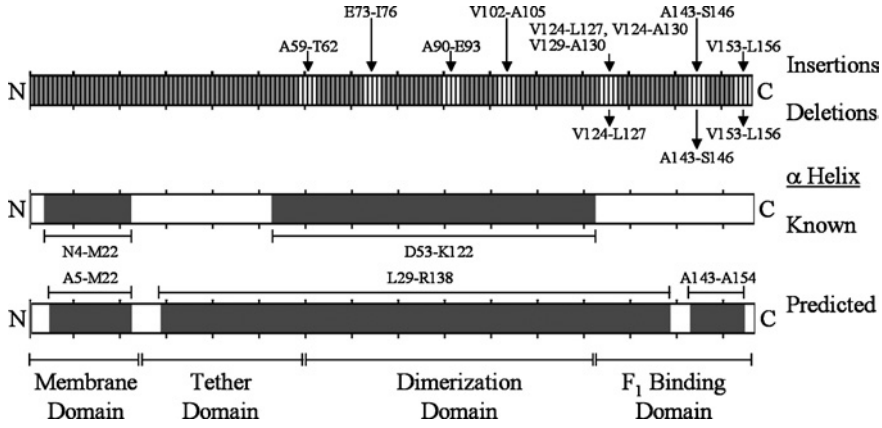

Fig. 2. Line drawing of the *b* subunit insertion and deletion mutations. On the top bar, the arrows (↓) indicate the positions of insertions (above the bar) and deletions (below the bar). The middle bar indicates areas of α-helical secondary structure based studies of model polypeptides (Dmitriev *et al*., 1999; Del Rizzo *et al*., 2002). The lower bar shows areas of predicted α-helical secondary structure.

Table I. Growth Properties and ATPase Activity in *b* Subunit Mutants

Strain/plasmid	Expressed *b* Subunit	Growth[1]	Membrane ATPase[2]
KM2/pKAM14	b	+++	1.47 ± 0.09
KM2/pBR3222	None	−	0.18 ± 0.04
KM2/pSC1	$b_{+ala59\rightarrow thr62}$	+++	1.15 ± 0.02
KM2/pSC2	$b_{+gln73\rightarrow ile76}$	+++	1.25 ± 0.05
KM2/pSC3	$b_{+ala90\rightarrow glu93}$	+++	1.44 ± 0.10
KM2/pSC4	$b_{+val102\rightarrow ala105}$	+++	1.27 ± 0.04
KM2/pDB20	$b_{\Delta val124\rightarrow ala130}$	−	0.18 ± 0.01
KM2/pDB22	$b_{+val124\rightarrow leu127}$	−	0.29 ± 0.01
KM2/pDB23	$b_{+val124\rightarrow ala130}$	(+)	0.18 ± 0.01
KM2/pDB24	$b_{(+val124\rightarrow ala130)x2}$ (+)	(+)	ND
KM2/pDB25	$b_{(+val124\rightarrow ala130)x3}$ (+)	(+)	ND
KM2/pDB21	$b_{+val129\rightarrow ala130}$	−	0.69 ± 0.09
KM2/pSC5	$b_{+ala143\rightarrow ser146}$	+++	1.22 ± 0.04
KM2/MMG1	$b_{\Delta ala143\rightarrow ser146}$	+++	ND
KM2/pTAM51	$b_{\Delta val153\rightarrow leu156}$	−	0.37 ± 0.04
KM2/pTAM52	$b_{+val153\rightarrow leu156}$	−	1.52 ± 0.07

[1]Growth on solid succinate-minimal A medium. Symbols: +++, colonies > 1.5 mm; −, no growth; (+) revertants.
[2]ATPase specific activity in membrane vesicles expressed as μM Pi/min/mg protein.

in biologically detectable phenotypes. Interestingly, altering the length of the segment between b_{ala130} and b_{leu156} at the carboxyl terminus, by constructing either the $b_{+ala143-ser146}$ insertion or the $b_{\Delta ala143-ser146}$ deletion, had no readily apparent effect. Both mutants yielded normal colony morphologies.

Enzymatic Activity

ATP hydrolysis activity in membrane vesicles prepared from the mutant strains was used as an assessment of assembly of stable F_1F_0 complexes and catalytic activity (Table I). In most instances, there was a correlation between the growth properties of a mutant and the level of membrane-associated ATPase activity. Only the carboxyl terminal truncation $b_{\Delta val153-leu156}$ mutant and the hydrophobic sequence mutants had greatly reduced levels of activity. The lone exception was that membranes from KM2/DB21 ($b_{val129-ala130}$) reproducibly showed intermediate amounts of membrane ATPase activity. This level of activity would normally be associated with membranes from a strain capable of slow growth on succinate minimal medium. The *in vivo* growth studies on selective medium were clearly negative (Table I), and there was no indication of phenotypic reversion during culture growth on rich medium for preparation of membrane fractions. Therefore, LDAO-stimulated activity was determined as an indication of coupling. For fully coupled F_1F_0 ATP synthase, LDAO treatment results in increased activity reflecting a release of F_1 from the influence of F_0. LDAO had no effect on F_1F_0 ATPase activity in the KM2/DB21 ($b_{val129-ala130}$) membranes (data not shown) suggesting that any F_1F_0 complexes assembled with the $b_{val129-ala130}$ subunit were not coupled.

Membranes prepared from insertion mutants at most sites displayed ATP-proton pumping activity approaching that observed in wild type membranes (Fig. 3(a)). In contrast, disruption of the hydrophobic sequence yielded no detectable ATP-driven proton translocation (Fig. 3(b)). This was true even in the KM2/pDB21 ($b_{val129-ala130}$) membranes confirming the absence of coupled activity. All membrane preparations were shown to have strong NADH-driven proton pumping activity (data not shown), so the negative proton translocation results could not be a consequence of excessive leakiness of the vesicle preparations.

Assembly of Stable F_1F_0

Immunoblot analyses were performed using an anti-*b* subunit antibody to investigate whether the recombinant *b* subunits were assembled into stable F_1F_0 complexes within the membranes. The *b* subunit is rapidly turned over outside the context of the intact F_1F_0 complex, so the strength of signal can be considered as an indication of the relative amount of complexes in the membrane. By using the high sensitivity ECL immuno-detection system and overexposing the blot, it was possible to see recombinant *b* subunits in all membrane preparations with the exception for the negative control KM2/pBR322 membranes (Fig. 4, lane 1). This included membranes derived from strains with altered hydrophobic sequences. However, using appropriate exposures and image analysis it was clear that *b* subunit levels were reduced in some mutant membrane preparations. The largest signal reduction was observed in KM2/DB20 ($b_{\Delta val124-ala130}$) membranes (Fig. 4, lane 9) where the intensity was only about 7% of the intensity of the wild type control. These results suggested a major failure to assemble stable enzyme complexes caused by either insertion or deletion into the hydrophobic sequence. In membranes from strain KM2/DB21, a much higher yield of $b_{+val129-ala130}$ subunit was readily apparent on the immunoblots suggesting that there was some assembly of F_1F_0 complexes in these membranes. However, as described above, F_1F_0 complexes containing $b_{+val129-ala130}$ subunits were fully uncoupled.

Since the hydrophobic sequence mutations resulted in major defects, we considered whether these defects would prevent the $b_{+val124-ala130}$ subunit from

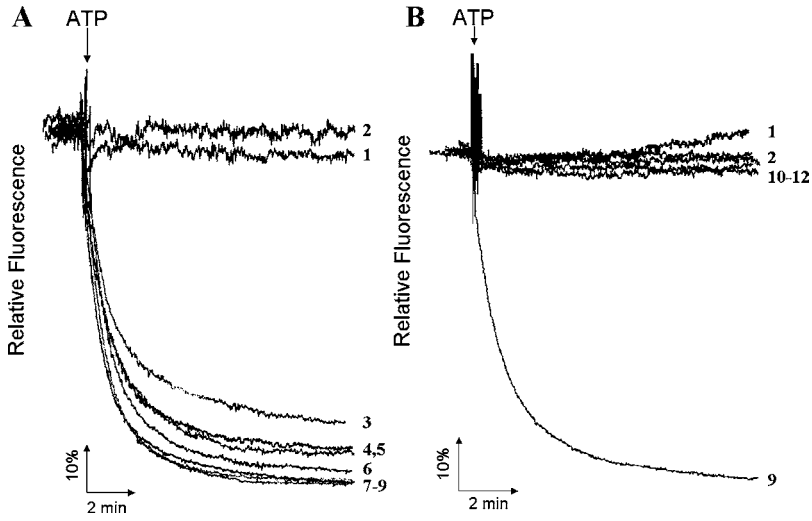

Fig. 3. ATP-driven energization of membrane vesicles prepared from *b* subunit mutant strains. Membranes were prepared from cells grown in rich medium and then assayed for proton pumping activity by monitoring fluorescence of ACMA following addition of ATP. Panel A. Membranes prepared from four codon insertion mutants. Panel B. Membranes of selected hydrophobic sequence mutants. Traces: 1, KM2/pBR322(Δb); 2, KM2/pDB22($b_{+\mathrm{val124-leu127}}$); 3, KM2/pSC4($b_{+\mathrm{val102-ala105}}$); 4, KM2/pSC5($b_{+\mathrm{ala146-ser146}}$); 5, KM2/pSC3($b_{+\mathrm{ala90-glu93}}$); 6, KM2/pSC1($b_{+\mathrm{ala59-thr62}}$); 7, KM2/pSC2($b_{+\mathrm{gln73-ile76}}$); 8, KM2/pTAM52($b_{+\mathrm{val153-leu156}}$); 9, KM2/pKAM14(*b*); 10, KM2/pDB20($b_{\Delta\mathrm{val124-ala130}}$); 11, KM2/pDB23($b_{+\mathrm{val129-ala130}}$);12, KM2/pDB23 ($b_{+\ \mathrm{val124-ala130}}$).

participating in dimerization with a normal *b* subunit for assembly of a peripheral stalk. This was accomplished by expressing both types of subunits into *E. coli* strain KM2 (Grabar and Cain, 2003, 2004). Plasmids pTAM38 ($b_{6his,+\mathrm{val124-ala130}}$) carrying the insertion mutation and an amino-terminal histidine-tag and pTAM46 ($b_{\mathrm{WT,V5}}$) with a V5-epitope tag (Grabar and Cain, 2004) were used in these experiments. The membranes were solubilized and F_1F_0 complexes containing at least one $b_{+\ \mathrm{val124-ala130}}$ subunit selected by Ni-resin chromatography. When control membranes from strain KM2(Δb)/pTAM38 ($b_{6\mathrm{his},+\mathrm{val124-ala130}}$) were studied no signal was seen in Western blots using an anti-*b* antibody (Fig. 5, lane 2). This indicated that the small number of F_1F_0 complexes assembled with homodimeric $b_{+\mathrm{val124-ala130}}$ peripheral stalks were not stable through solubilization and purification. A second important control using membranes from cells expressing only the $b_{\mathrm{WT,V5}}$ subunit demonstrated that F_1F_0 complexes lacking a histidine-tagged subunit were eliminated by the Ni-CAM purification step (Fig. 5, lane 1). A completely different result was obtained using membrane vesicles from strain KM2/pTAM38 ($b_{6\mathrm{his},+\mathrm{val124-ala130}}$)/pTAM46 ($b_{\mathrm{WT,V5}}$). Western analysis of the material obtained from Ni-resin chromatography yielded strong signals detected with both anti-*b* subunit and anti-V5 antibodies (Fig. 5, lane 4). This result could only be obtained if F_1F_0 complexes existed with a heterodimer $b_{6\mathrm{his},+\mathrm{val124-ala130}}/b_{\mathrm{WT,V5}}$ peripheral stalk. Moreover, the $b_{\mathrm{WT,V5}}$ subunit must have stabilized the $b_{6\mathrm{his},+\mathrm{val124-ala130}}$ in F_1F_0 complexes through the purification protocol. The heterodimeric complexes were most likely functional. When KM2/pTAM38

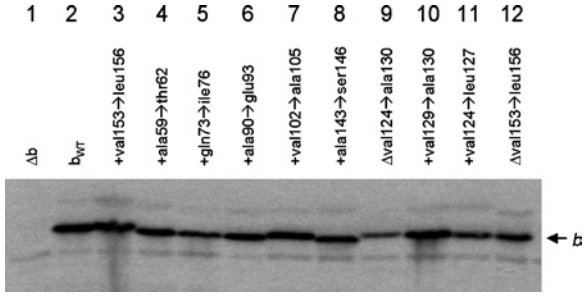

Fig. 4. Immunoblot of membranes prepared from *b* subunit mutants. Membrane proteins (20 μg) were separated on a 15% *bis*-acrylamide gel and transferred to nitrocellulose membrane. Immunodetection using an anti-*b* subunit polyclonal antibody was performed as described (Grabar and Cain, 2003). This autoradiogram was exposed for 1 h for maximum sensitivity to weaker signals. The mutations in the *b* subunit are labeled above each lane.

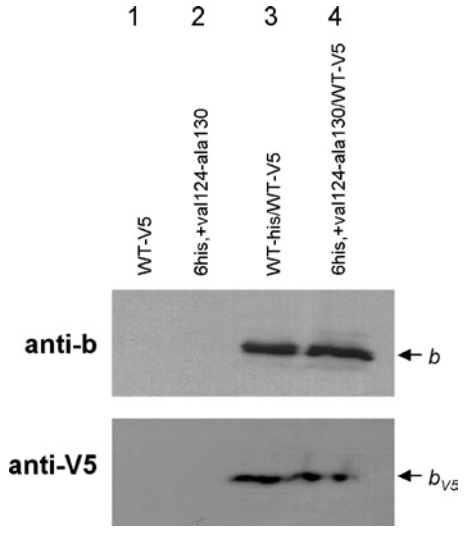

Fig. 5. Ni-resin purification of F_1F_0 complexes with a heterodimeric peripheral stalk. Membranes from strains expressing recombinant *b* subunits were prepared. The membranes were solubilized in 0.2% tegamineoxide WS-35 and selected by Ni-resin purification (Grabar and Cain, 2003). The complexes were run on a 15% bis-acrylamide gel and transferred to nitrocellulose membrane. Subunit *b* proteins in Ni-resin purified F_1F_0 complexes were detected with either: Panel A, an anti-*b* subunit polyclonal antibody; or Panel B, the anti-V5 mouse monoclonal antibody. The *b* subunits expressed are indicated above the panels.

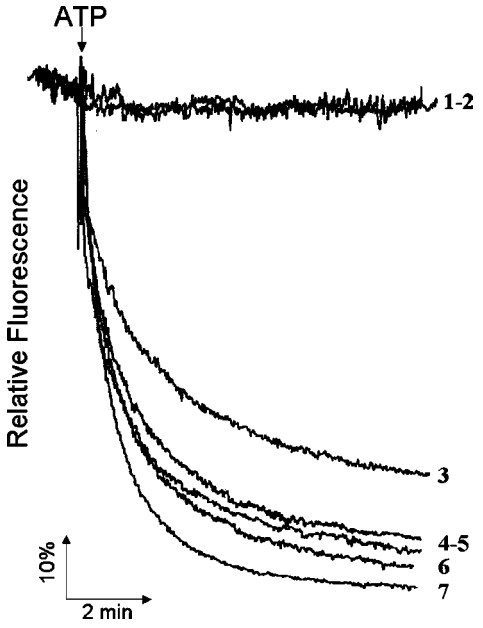

Fig. 6. ATP-driven energization of membrane vesicles prepared from cells expressing combinations of *b* subunits. Membranes were prepared from cells grown in rich medium and assayed for ATP-driven proton pumping activity by monitoring fluorescence of ACMA. Traces: 1, KM2/pBR322(Δ*b*); 2, KM2/pTAM38($b_{6his,+val124-ala130}$); 3, KM2/pTAM37($b_{6his,WT}$); 4, KM2/pTAM46($b_{WT,V5}$)/pTAM38($b_{6his,+val124-ala130}$); 5, KM2/pTAM37 ($b_{6his,WT}$)/pTAM46($b_{WT,V5}$); 6, KM2/pTAM46($b_{WT,V5}$); 7, KM2/pKAM14 (*b*).

($b_{6his,+val124-ala130}$)/pTAM46 ($b_{WT,V5}$) membrane vesicles were studied for ATP-driven proton pumping activity, the level of activity was nearly identical to membranes from KM2/pTAM37($b_{6his,WT}$)/pTAM38($b_{WT,V5}$) and greater than the activity observed in KM2/pTAM37($b_{6his,WT}$) membranes (Fig. 6).

DISCUSSION

Widely disparate phenotypes have been reported for mutations altering the length of the *b* subunit. Our earlier work showed that shortening or lengthening the tether domain by seven amino acids yielded abundant levels of fully active F_1F_0 ATP synthase (Sorgen *et al*., 1998, 1999; Grabar and Cain, 2003), and larger deletions and insertions were accommodated within functional enzymes. In contrast, truncating the carboxyl-terminus by as few as four amino acids resulted in a catastrophic failure in the enzyme complex (Takeyama *et al*., 1988; McLachlin *et al*., 1998; Grabar and Cain, 2004). Not surprisingly, the position of the mutations were important and not merely the length of the *b* subunit. Here we have surveyed the dimerization and F_1 binding domains of the *b* subunit by insertion and deletion mutagenesis. Only the hydrophobic sequence, val-124 to ala-132, at the junction between domains and the carboxyl-terminal segment of the *b* subunit proved to be essential structural features. This is in agreement with the literature (Dunn *et al*., 2000a,c). The insertion of four codons into the hydrophobic sequence in the $b_{6his,+val124-ala130}$ subunit caused a major assembly/stability defect when expressed alone. However, the defective subunit could be assembled with the normal $b_{WT,V5}$ subunit into a heterodimeric peripheral stalk yielding an apparently functional F_1F_0 ATP synthase.

The *b* subunit hydrophobic sequence has long been thought to participate in subunit–subunit interactions important for forming the F_1F_0 complex. Like the insertions and deletions in this area reported here, the $b_{ala124\rightarrow asp}$ and $b_{gly131\rightarrow asp}$ mutations resulted in apparent defects in assembly (Porter *et al*., 1985; Howitt *et al*., 1996). Both the properties of the $b_{ala124\rightarrow asp}$ mutation and the capacity to form disulfide bridges between *b* subunits with cysteines introduced from the hydrophobic sequence at position 124 through the carboxyl terminus (McLachlin and Dunn, 1997) suggested that the F_1 binding domain might contribute to the formation of the peripheral stalk b_2 dimer. However, Dunn *et al*. (2000b) later showed that the $b_{ala124\rightarrow asp}$ substitution caused a structural defect

apparently altering the carboxyl terminal domain in such a way as to prevent appropriate interactions between the b_2 dimer and F_1. The disruptions of protein–protein interactions resulting from the $b_{+ala143-ser146}$ insertion and $b_{\Delta ala143-ser146}$ deletion were comparatively mild. If a hydrophobic sequence defect was propagated linearly along the b subunit to the site of the b–δ interaction, then the $b_{+ala143-ser146}$ and $b_{\Delta ala143-ser146}$ mutations would have been expected to have stronger effects. Instead, it seems more likely that the hydrophobic sequence has a direct impact on the conformation necessary for the b--δ interaction, perhaps through a tertiary structure interaction. Dunn *et al*. (2000a) have proposed a folded structure at the carboxyl terminus of the b subunit based on hydrodynamic properties of the b_{sol} polypeptide with a carboxyl terminal deletion. It is noteworthy that a hydrophobic sequence mutation, such as $b_{+val124-leu127}$, did not yield biochemical properties identical to the carboxyl terminal $b_{\Delta val153-leu156}$ deletion. Although both eliminated F_1F_0 ATPase function, a considerably higher amount of the $b_{\Delta val153-leu156}$ subunit was found in the membranes. This would suggest that the structural defect in the $b_{+val124-leu127}$ protein affects complex assembly in some manner beyond merely interfering with the known b--δ interaction.

The stabilization of the $b_{6his,+val124-ala130}$ subunit by a wild type b in the F_1F_0 complex has broader implications for complex assembly. First, as has been observed in our studies of the tether domain (Grabar and Cain, 2003), the two b subunits need not be in perfect register along their entire lengths to form a functional b_2 dimer. More importantly, although complex assembly was severely impaired by a $b_{6his,+val124-ala130}$ homodimer, it was clear that insertion of additional sequence into a single b subunit in a heterodimeric stalk did not block assembly of an F_1F_0 complex. The corollary to that interpretation is that the $b_{wt,V5}$ subunit made the necessary contacts with F_1, or alternatively, drove the defective $b_{6his,+val124-ala130}$ into a productive conformation. Collectively these observations provide independent evidence for the hypothesis that the two b subunits perform differing functions within the peripheral stalk of F_1F_0 ATP synthase (Grabar and Cain, 2004).

ACKNOWLEDGMENTS

The authors wish to thank Cortney Bouldin and Megan Greenlee for their participation in specific experiments presented here. We also wish to thank Dr. Gabriela Deckers-Hebestreit for contributing the anti-b subunit antibodies. This work supported by PHS grant RO1 GM43495 (to BDC).

REFERENCES

Boyer, P. D. (2002). *J. Biol. Chem.* **277**, 39045–39061.
Cain, B. D. (2000). *J. Bioenerg. Biomembr.* **32**, 365–371.
Caviston, T. L., Ketchum, C. J., Sorgen, P. L., Nakamoto, R. K., and Cain, B. D. (1998). *FEBS Lett.* **429**, 201–206.
Del Rizzo, P. A., Bi, Y., Dunn, S. D., and Shilton, B. H. (2002). *Biochemistry* **41**, 6875–6884.
Dmitriev, O., Jones, P. C., Jiang, W., and Fillingame, R. H.. (1999). *J. Biol. Chem.* **274**, 98–15604.
Dunn, S. D., Bi, Y., and Revington, M. (2000a). *Biochim. Biophys. Acta* **1459**, 521–527.
Dunn, S. D., McLachlin, D. T., and Revington, M. (2000b). *Biochim. Biophys. Acta* **1458**, 356–363.
Dunn, S. D., Revington, M., Cipriano, D. J., and Shilton, B. H. (2000c). *J. Bioenerg. Biomembr.* **32**, 347–355.
Gardner, J. L., and Cain, B. D. (1999). *Arch. Biochem. Biophys.* **361**, 302–308.
Grabar, T. B., and Cain, B. D. (2003). *J. Biol. Chem.* **278**, 27873–27878.
Grabar, T. B., and Cain, B. D. (2004). *J. Biol. Chem.* **279**, 31205–31211.
Hardy, A. W., Grabar, T. B., Bhatt, D., and Cain, B. D. (2003). *J. Bioenerg. Biomembr.* **35**, 389–397.
Howitt, S. M., Rodgers, A. J. W., Jeffrey, P. D., and Cox, G. B. (1996). *J. Biol. Chem.* **271**, 7038–7042.
McCormick, K. A., and Cain, B. D. (1991). *J. Bacteriol.* **173**, 7240–7248.
McLachlin, D. T., Bestard, J. A., and Dunn, S. D. (1998). *J. Biol. Chem.* **273**, 15162–15168.
McLachlin, D. T., and Dunn, S. D. (1997). *J. Biol. Chem.* **272**, 21233–21239.
McLachlin, D. T., and Dunn, S. D. (2000). *Biochemistry* **39**, 3486–3490.
Miller, J. H. (1992). In *A Short Course in Bacterial Genetics*, Cold Spring Harbor Laboratory Press, Cold Spring Harbor, New York, pp. 25.3–25.5.
Motz, C., Hornung, T., Kersten, M., McLachlin, D. T., Dunn, S. D., Wise, J. G., and Vogel, P. D. (2004). *J. Biol. Chem.* **279**, 49074–49081.
Noji, H., and Yoshida, M. (2001). *J. Biol. Chem.* **276**, 1665–1668.
Ogilvie, I., Aggeler, R., and Capaldi, R. A. (1997). *J. Biol. Chem.* **272**, 16652–16656.
Porter, A. C. G., Kumamoto, C., Aldape, K., and Simoni, R. D. (1985). *J. Biol. Chem.* **260**, 8182–8187.
Senior, A. E., Nadanaciva, S., and Weber, J. (2002). *Biochim. Biophys. Acta* **1553**, 188–211.
Smith, P. K., Krohn, R. I., Hermanson, G. T., Mallia, A. K., Gartner, F. H., Provenzano, M. D., Fujimoto, E. K., Goeke, N. M., Olson, B. J., and Klenk, D. C. (1985). *Anal. Biochem.* **150**, 76–85; erratum 1987. *Anal. Biochem.* **163**, 279.
Sorgen, P. L., Caviston, T. L., Perry, R. C., and Cain, B. D. (1998). *J Biol. Chem.* **273**, 27873–27878.
Sorgen, P. L., Bubb, M. R., and Cain, B. D. (1999). *J Biol. Chem.* **274**, 36261–36266.
Takeyama, M., Noumi, T., Maeda, M., and Futai, M. (1988). *J. Biol. Chem.* **263**, 16106–16112.
Weber, J., Muharemagic, A., Wilke-Mounts, S., and Senior, A. E. (2003). *J. Biol. Chem.* **278**, 13623–13626.
Weber, J., Wilke-Mounts, S., Nadanaciva, S., and Senior, A. E. (2004). *J. Biol. Chem.* **279**, 25673–25679.
Wilkens, S. (2000). *J. Bioenerg. Biomembr.* **32**, 333–339.